Magnon Scattering of Polarized Neutrons by the Diffraction Method: Measurements on Magnetite*

H. A. ALPERIN
U. S. Naval Ordnance Laboratory, Silver Spring, Maryland and Brookhaven National Laboratory, Upton, New York
AND
O. STEINSVOLL,† R. NATHANS, AND G. SHIRANE
Brookhaven National Laboratory, Upton, New York

(Received 25 August 1966)

The acoustic branch of the spin-wave spectrum of a ferromagnet may be measured by the inelastic scattering of neutrons. It is shown that when polarized neutrons are employed in conjunction with the diffraction method, data may be secured over a sufficient range of the magnon wave vector q to test the applicability of the Heisenberg model. The procedures for utilizing this technique are described. In particular, the methods used for correcting for the instrumental resolution and for converting the data into the form of a dispersion relation are explained. This procedure has been applied to a study of Fe_3O_4 at room temperature for values of q/q_{max} up to ~ 0.3. The results are in very good agreement with measurements by direct energy analysis and with the predictions of the Heisenberg theory. A value of 2.35×10^{-3} eV is obtained for the exchange integral. Additional data taken at 77°K show that the dispersion relation in magnitite is substantially the same in the high- and low-temperature phases (i.e., above and below the A-B site ordering transition at 119°K).

I. INTRODUCTION

THE inelastic scattering of neutrons by the spin-wave excitations of a magnetic solid provides a unique method for determining the complete set of dispersion relations [energy $\hbar\omega(q)$ as a function of the wave vector q] for these excitations. In principle, all branches may be measured for a value of q up to its value at the zone boundary. There are four methods whereby the dispersion relation may be measured: direct energy analysis of the inelastically scattered neutrons, the so-called diffraction method, neutron small-angle scattering[1] and spin-wave resonance.[2] Small-angle scattering only samples the dispersion relation at very small q values where the dependence on q is quadratic for a ferromagnet. Until now spin-wave resonance has been similarly restricted, although recently Weber and Tannenwald[3] have refined this technique in order to measure the departure from quadratic behavior in Permalloy where high quality films can be prepared. Energy analysis is the only method which allows measurements to be performed up to the zone boundary and is also essential for observing the higher energy modes. It however, requires a very high flux reactor and a rather complicated experimental arrangement. The diffraction method which is simpler to employ is useful for observing the lowest (acoustic) spin-wave mode in the approximate range $0.05<q/q_{max}<0.35$ and in this range may have an accuracy which is in many cases equal to or superior to that obtained heretofore by energy analysis.

Spin-wave dispersion relations have been determined by energy analysis for Fe_3O_4,[4] MnO,[5] MnF_2,[6] and Co.[7] With the diffraction method, measurements have been made over a wide range of q values for Fe_3O_4,[8] Fe_7S_8,[9] Co,[10] Co and Ni,[11,12] Fe,[13] and hexagonal Co.[14] Only in the last three references cited have actual dispersion curves been presented. These papers have used the methods to be presented here.

The present investigation was undertaken as the first step in a program to use the diffraction method to study dispersion relations in the ferromagnetic metals. In particular, it is expected that by making measurements over a wide range of q values one may detect possible

* Work performed under the auspices of the U. S. Atomic Energy Commission.

† Guest scientist from Institutt for Atomenergi, Kjeller, Norway.

[1] See R. D. Lowde, J. Appl. Phys. **36**, 884 (1965).

[2] See, e.g., T. G. Phillips and H. M. Eosenberg, in *Proceedings of the International Conference on Magnetism, Nottingham, 1964* (The Institute of Physics and The Physical Society, London, 1965), p. 306; M. Nisenoff and R. W. Terhune, J. Appl. Phys. **36**, 732 (1965).

[3] R. Weber and P. E. Tannenwald, J. Appl. Phys. **37**, 1058 (1966).

[4] B. N. Brockhouse and H. Watanabe, *Inelastic Scattering of Neutrons in Solids and Liquids II* (International Atomic Energy Agency, Vienna, 1963), p. 297.

[5] M. F. Collins, in *Proceedings of the International Conference on Magnetism, Nottingham, 1964* (The Institute of Physics and The Physical Society, London, 1965), p. 319.

[6] G. G. Low, A. Okazaki, R. W. H. Stevenson, and K. C. Turberfield, J. Appl. Phys. **35**, 998 (1964).

[7] R. N. Sinclair and B. N. Brockhouse, Phys. Rev. **120**, 1638 (1960).

[8] T. Riste, K. Blinowski, and J. Janik, J. Phys. Chem. Solids **9**, 153 (1959).

[9] A. Wanic, J. Phys. Radium **25**, 627 (1964).

[10] E. Frikkee and T. Riste, in *Proceedings of the International Conference on Magnetism, Nottingham, 1964* (The Institute of Physics and The Physical Society, London, 1965), p. 299.

[11] T. Riste, G. Shirane, H. A. Alperin, and S. J. Pickart, J. Appl. Phys. **36**, 1076 (1965).

[12] S. J. Pickart, H. A. Alperin, V. J. Minkiewicz, R. Nathans, G. Shirane, and O. Steinsvoll, Phys. Rev. (to be published).

[13] G. Shirane, R. Nathans, O. Steinsvoll, H. A. Alperin, and S. J. Pickart, Phys. Rev. Letters **15**, 146 (1965).

[14] H. A. Alperin, O. Steinsvoll, G. Shirane, and R. Nathans, J. Appl. Phys. **37**, 1052 (1966).

departures from Heisenberg behavior. In order to accomplish this it is necessary to work out details of the correction for instrumental resolution and to be able to deduce the dispersion law from the raw data. The study of magnetite affords the opportunity to obtain results by the diffraction method which may be directly compared with data taken by direct energy analysis. Riste[15] has presented some results on the temperature dependence of the magnon scattering in Fe_3O_4 which did indicate a consistency between the two methods. These data however were taken only for small q values. Since the entire acoustic branch has been measured for Fe_3O_4 by Brockhouse and Watanabe[4] by energy analysis, measurements by the diffraction method up to moderate q values make it possible to directly compare dispersion relations obtained by the two methods thereby including any systematic errors which might arise in the corrections for instrumental resolution or in the process of data reduction. In addition, the calculations of Kaplan[16] and Glasser and Milford[17] for Fe_3O_4 afford an opportunity to compare our measurements with theory as well. A final motivation for this study lies in the discrepancy by a factor of 6 which exists between the value of the exchange consant determined by Kouvel[18] from low-temperature specific-heat measurements and that determined by room-temperature neutron scattering. It was of interest therefore to perform some magnon scattering measurements at a temperature below the ordering temperature of 119°K to see if there is any change in the dispersion law below this temperature.

At room temperature the ferrimagnet Fe_3O_4 has the inverse spinel structure in which the eight tetrahedral (A) sites are occupied by Fe^{3+} ions and the sixteen octahedral (B) sites are occupied randomly by Fe^{2+} and Fe^{3+} ions. Neutron-diffraction measurements by Shull *et al.*[19] have shown that the A- and B-site moments are aligned oppositely. This antiferromagnetic exchange interaction J_{AB} is taken to be the dominant interaction in this material. Below 119°K the Fe^{2+} and Fe^{3+} moments on the B sites order into mutually perpendicular rows thus imposing orthorhombic symmetry on the structure.

The diffraction method, first described by Elliott and Lowde[20] was first applied to Fe_3O_4 by Riste *et al.*[8] They employed a white neutron beam in order to obtain the highest possible flux. Although there is some scatter in their experimental points (due most likely to the difficulty in correcting for the instrumental resolution), nevertheless if the dispersion law over the range of q is assumed to be quadratic, $\hbar\omega=\alpha q^2\hbar^2/2m$, then they deduced a value $\alpha=225$ and a corresponding value for the exchange interaction $J_{AB}=2\times10^{-3}$ eV. The first work on the scattering of polarized neutrons by spin waves was done by Ferguson and Sáenz[21] who verified qualitatively the polarization dependence to be expected[22] from the one-magnon zero-phonon scattering by an exchange-coupled lattice. Samuelsen *et al.*[23] applied this method to Fe_3O_4 under somewhat better experimental conditions. They investigated further experimental details and measured three points, which were consistent with the value $J_{AB}=2.3\times10^{-3}$ eV obtained by Brockhouse and Watanabe[4] from their direct-energy-analysis measurements. Recently, Fersuson *et al.*[24] have made some further measurements on Fe_3O_4 using the diffraction method with polarized neutrons. They obtain $\alpha=234\pm20$ upon assuming a quadratic dispersion law.

The theoretical work on the magnon dispersion relation for Fe_3O_4 began with Kouvel[25] who took into account nearest-neighbor AA, BB, and AB interactions to derive a q^2 dependence for the energy of the acoustic branch in the limit of small q. Independently, Kaplan[16] derived the energy spectra for a normal spinel. Glasser and Milford[17] have extended the Kouvel work of the inverse spinel to higher orders in q^2 dependence.

II. THEORY

A. Ferrimagnetic Spin Waves

A monoatomic Heisenberg ferromagnet possesses only a single (acoustic) branch in its spectrum. Linear spin-wave theory then yields the following expression for its energy[26]:

$$\hbar\omega=2S\sum_{\mathbf{r}}J(\mathbf{r})[1-e^{\mathbf{q}\cdot\mathbf{r}}]+\hbar\omega_0 \qquad (1)$$

where $J(\mathbf{r})$ is the exchange interaction between two atoms a distance $\mathbf{r}$ apart, S is the spin, and $\hbar\omega_0$ represents the energy gap (at $q=0$) due to the effects of anisotropy and an applied external field. If it is further assumed that only nearest-neighbor interactions J_1 are effective, then for example for a body-centered cubic lattice (lattice constant, a) with $\mathbf{q}$ along the [100] direction we would have the following simple expression for the dispersion relation:

$$\hbar\omega=16J_1S[1-\cos(qa/2)]. \qquad (2)$$

At small values of q, the energy is proportional to q^2.

[15] T. Riste, J. Phys. Soc. Japan **17**, Suppl. B-III, 60 (1962).
[16] T. S. Kaplan, Phys. Rev. **109**, 782 (1958).
[17] M. L. Glasser and F. J. Milford, Phys. Rev. **130**, 1783 (1963).
[18] J. S. Kouvel, Phys. Rev. **102**, 1489 (1956).
[19] C. G. Shull, E. Wollan, and W. Koehler, Phys. Rev. **84**, 912 (1951).
[20] R. J. Elliott and R. D. Lowde, Proc. Roy. Soc. (London) **A230**, 46 (1955).
[21] G. A. Ferguson and A. W. Sáenz, J. Phys. Chem. Solids **23**, 117 (1962).
[22] A. W. Sáenz, Phys. Rev. **125**, 1940 (1962).
[23] E. J. Samuelsen, T. Riste, and O. Steinsvoll, Phys. Letters **6**, 47 (1963).
[24] G. A. Ferguson, A. W. Sáenz, and A. D. Anderson, Report of Naval Research Laboratory Progress, 1965, p. 10 (unpublished).
[25] J. S. Kouvel, Cruft Laboratory, Harvard, Technical Report No. 210, 1955 (unpublished), but see Ref. 17 for a summary.
[26] See, e.g., C. Kittel, *Quantum Theory of Solids* (John Wiley & Sons, Inc., New York, 1963).

The spinel structure of magnetite consists of six interpenetrating face-centered cubic lattices, two of A sites and four of B sites and hence its spin-wave spectrum will contain six branches. However, one expects the lowest acoustic branch to have a form qualitatively similar to Eq. (1). Physically, this branch arises from in-phase precessional motion of the A and B sublattices. Since the dependence on the direction of the wave vector $\mathbf{q}$ would be barely detectable only close to the zone boundary,[17] we may conveniently take $|\mathbf{q}|=q_x\equiv q$ and $q_y=q_z=0$ to obtain a simple expression for the dispersion relation of the acoustic branch from the equations given in Ref. 17 for the case $J_{AA}=J_{BB}=0$, $J_{AB}\neq 0$; namely,

$$\hbar\omega/12J_{AB}=-1+\tfrac{1}{2}\{49-5[\cos(3aq/8)+2\cos(aq/8)]^2\}^{1/2}. \quad (3)$$

B. The Scattering of Neutrons by Spin Waves

The fundamental formula for the scattering cross section for unpolarized neutrons was given sometime ago by Elliott and Lowde.[20] Aside from details which are unimportant for our present purposes, the cross section depends on delta functions of the energy and momentum, i.e., the intensity of the inelastically scattered neutrons is zero unless energy and momentum are conserved:

$$(\pm)\hbar\omega=(\hbar^2/2m)(k_f^2\pm k_i^2) \quad (4)$$

$$\mathbf{k}_i+2\pi\boldsymbol{\tau}-\mathbf{q}=\mathbf{k}_f. \quad (5)$$

Here, $\hbar\omega$ is the magnon energy (the + sign denotes magnon annihilation and the − sign, magnon creation), m is the neutron mass, $\mathbf{k}_f$ and $\mathbf{k}_i$ are the final (i.e., scattered) and incident neutron wave vectors, $\boldsymbol{\tau}$ is the reciprocal lattice vector (i.e., $2\pi\boldsymbol{\tau}\hbar$ is the momentum taken up by the crystal lattice), and $\mathbf{q}$ is the magnon wave vector. Equations (4) and (5) together with the dispersion law, $\hbar\omega=\hbar\omega(q)$ assumed to be a continuous function, uniquely determine the scattering surface. If one considers a dispersion relation quadratic in q,

$$\hbar\omega=(\hbar^2/2m)\alpha q^2\equiv Dq^2 \quad (6)$$

(D is commonly called the magnetic stiffness constant in analogy with the corresponding stiffness coefficient for the energy of an elastic solid) it can then be shown[27] that the scattering surface is exactly a sphere. The geometry of the situation is shown in Fig. 1. The wave vector of the scattered neutron $\mathbf{k}_f$ may terminate anywhere on the scattering surface so that a horizontal scan of the neutron counter will yield an intensity profile with a rather flat top and sharp cutoffs on the sides. The cutoff corresponds to $\mathbf{k}_f$ tangent to the scattering surface and defines the angle $\Gamma/2$ as shown in the figure.[28] The vector $\mathbf{k}_1\equiv\mathbf{k}_i+2\pi\boldsymbol{\tau}$, is completely determined by a knowledge of the incident-neutron wavelength ($|k_i|=2\pi/\lambda$) and the angle $\Delta\varphi$ by which the crystal is misset from the Bragg position. The angle Γ is small so that to a first approximation $k_f\approx k_1$ and then

$$\hbar\omega\approx(\pm)(\hbar^2/2m)(k_1^2-k_i^2) \quad \text{and} \quad q\approx\Gamma k_1/2. \quad (7)$$

As $\Delta\varphi$ departs from zero, k_1^2 deviates more and more from k_i^2 corresponding to an increase in the magnon energy. Since the dispersion law predicts an increase in q for increasing energy, this then means that to a given point on the dispersion curve in $(\hbar\omega,q)$ space there corresponds a sphere with a given diameter and location (specified by $\Delta\varphi$) in our experimental scattering space. As $\Delta\varphi$ is increased, the diameter of the sphere increases and points further along the dispersion curve (i.e., for larger q values) are measured. Measurements of Γ as a function of $\Delta\varphi$ then constitute the results of the diffraction method measurements. As explained in Ref. 27, a useful way to plot the data is $\sin^2(\Gamma/2)$ versus k_i^2/k_1^2 since for the spherical scattering surface (i.e., the quadratic dispersion law) a straight line will result.

The use of polarized neutrons in conjunction with the diffraction method provides a very simple means for eliminating several unwanted contaminants from the inelastic magnon scattering. As shown by Sáenz[22] the polarization dependence of the differential scattering cross section for one-magnon, zero-phonon scattering is given by

$$d\sigma/d\Omega=[1+(\hat{e}\cdot\hat{m})^2-2(\pm)(\mathbf{P}_0\cdot\hat{e})(\hat{m}\cdot\hat{e})]\cdot G(\omega_q), \quad (8)$$

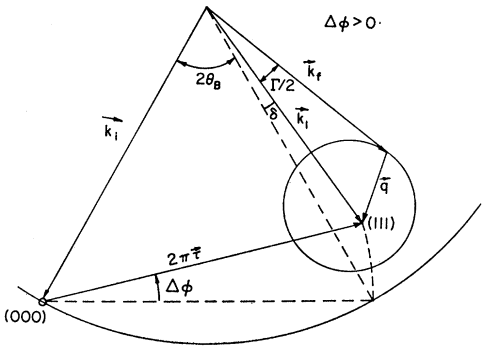

FIG. 1. Scattering geometry in reciprocal space. $\mathbf{k}_i$ is the wave vector of the incident neutron, and $2\pi\boldsymbol{\tau}$ is the reciprocal lattice vector. The circle (drawn here much larger than true scale since, as shown in Table I, $\Gamma/2$ is never greater than 2.5°) is the projection of a spherical scattering surface which holds in the case of a quadratic dispersion law $\hbar\omega\propto q^2$. The crystal is shown misset an angle $\Delta\varphi>0$ from the (111) Bragg position (Bragg angle θ_B) corresponding to magnon creation. $\mathbf{k}_f$ and $\Gamma/2$ are defined in the text.

[27] Institutt for Atomenergi, Kjeller, Norway, Annual Technical Report No. 3, 1963 (unpublished).

[28] Actually, if there were no effects due to instrumental resolution, then a horizontal scan of the scattering surface with a counter sufficiently tall to accept all scattered neutrons would yield a rectangular profile. This comes about simply because slices of constant width along a sphere yield equal surface areas. One must also assume that the q vectors are populated uniformly over the surface.

where the unit scattering vector

$$\hat{e}=(\mathbf{k}_i-\mathbf{k}_f)/|k_i-k_f|\,. \tag{9}$$

$\mathbf{P}_0$ is the polarization vector of the incoming beam,[29] $\hat{m}$ is a unit vector in the direction of the magnetization of the sample, $G(\omega_q)$ is a factor independent of $\mathbf{P}_0$ and $\hat{m}$ and the + and − signs denote magnon annihilation and creation as before. Now in addition to magnon scattering there may also be scattering present due to phonons, magnetovibrational scattering and magnetic elastic scattering. The first two may be written[30]

$$d\sigma/d\Omega=b_v^2+2b_vP_v(\mathbf{P}_0\cdot\mathbf{Q})+P_v^2Q^2, \tag{10}$$

where b_v^2 is the phonon scattering cross section, P_v^2 is the magnetovibrational scattering cross section, and $\mathbf{Q}\equiv\hat{e}(\hat{e}\cdot\hat{m})-\hat{m}$. The desired experimental arrangement is the one in which $\hat{e}\cdot\hat{m}=1$ so that $\mathbf{Q}=0$ and the magnetovibrational scattering is eliminated. In addition, the ordinary magnetic elastic scattering also vanishes[31] so that we are left with the pure phonon scattering. Now if the experimental setup is further arranged so that $\mathbf{P}_0\cdot\hat{e}=1$ then if the scattering arising from incident neutrons of one polarization state ($P_0=+1$) subtracted from that with the polarization reversed ($P_0=-1$) it is clear that the phonon contribution is subtracted and pure magnon scattering remains.

III. EXPERIMENTS

These experiments were performed at the Brookhaven graphite reactor on a large (25-mm×12-mm×6-mm-thick) natural single crystal of Fe_3O_4. The incident neutron wavelength was 1.05 Å. The polarized beam was obtained by Bragg scattering from a magnetized $Co_{0.92}$ $Fe_{0.08}$ single crystal.[31] The measurements were made in the vicinity of the (111) Bragg reflection so that to within a few degrees the scattering vector $\hat{e}$ (for the inelastic process) is along the [111] direction. By fixing the crystal in a permanent magnet with the field ($H\sim3000$ G) always in the [111] direction the condition $\hat{e}\cdot\hat{m}=1$ is very nearly satisfied. However, since $\hat{e}$ is in a horizontal plane and $\mathbf{P}_0$ for the beam as it leaves the monochromator is in a vertical direction, in order to insure $\mathbf{P}_0\cdot\hat{e}=1$ it was necessary to rotate the polarization of the neutron beam through 90°. This was accomplished simply by having the beam leave the vertical guide field of approximately 200 G and then perform an adiabatic turn in air, a distance of about 3 in., to a horizontal guide field of similar strength. (The loss in beam polarization due to the turn was only a few percent.) Transmission measurements through the magnetite crystal indicated that the beam suffered a depolarization of about 36% in passing from the monochromator through the sample. Although this is a rather large amount of depolarization, for practical purposes it in fact affects the final measurements very little. This is so because first, only the depolarization which takes place *before* scattering is effective in reducing the polarization dependence (i.e., in this case $P_{\text{eff}}=0.82$). Furthermore, if we note from Eq. (8) that for the optimum experimental arrangement, $d\sigma/d\Omega\propto1-P_{\text{eff}}$ then a figure of merit for the polarization efficiency of the experiment (for $\Delta\varphi>0$) is

$$\left[\frac{\text{OFF-ON}}{\text{OFF}}\right]=\frac{(1+.82)-(1-.82)}{1+.82}=\frac{1.64}{1.82}=90\% \tag{11}$$

Thus in spite of the rather high depolarization present, the over-all adverse effect is minimal.

For a fixed value of the misset angle $\Delta\varphi$ of the crystal from the Bragg position, data were collected as the counter was scanned across the scattering surface. The data for one misset angle is shown in Fig. 2. Note that the "ON" data are apparently flat, indicating as explained above that the effect of depolarization is hardly noticeable. Several scans for different missettings are shown in Fig. 3 where the plotted points are the difference in intensities for the two states of neutron polarization. It is clear that the effect of the instrumental resolution becomes quite important for small $\Delta\varphi$'s. For large misset angles, the ideal rectangular shape of the profile becomes apparent.

The bulk of the data was taken at room temperature but a few measurements were made at 77°K as well, where an electromagnet providing fields up to 10 000 G was used to magnetize the crystal which was contained

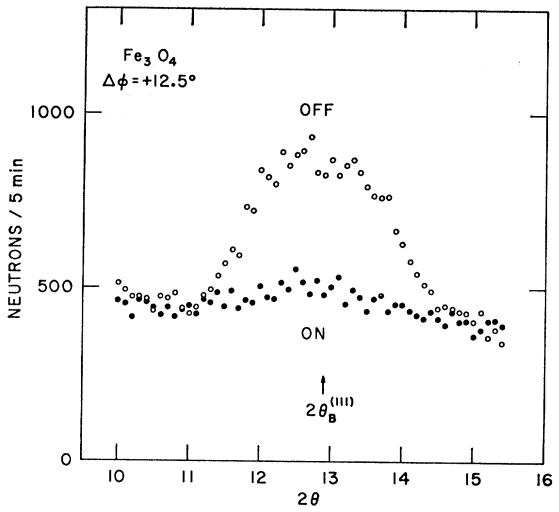

FIG. 2. Scan of the neutron counter across the scattering surface with the crystal fixed at a misset angle of 12.5° from the Bragg position. The closed points labeled "ON" and the open points labeled "OFF" refer to data taken with opposite states of incident neutron polarization.

[29] P_0 can take on the value +1 or −1. We refer to these states as "OFF" or "ON," corresponding to whether an rf coil which flips the neutron spin is energized or not.

[30] O. Steinsvoll, Institutt for Atomenergi, Kjeller, Report KR-65, 1963 (unpublished).

[31] R. Nathans, C. G. Shull, G. Shirane, and A. Andresen, J. Phys. Chem. Solids **10**, 138 (1959).

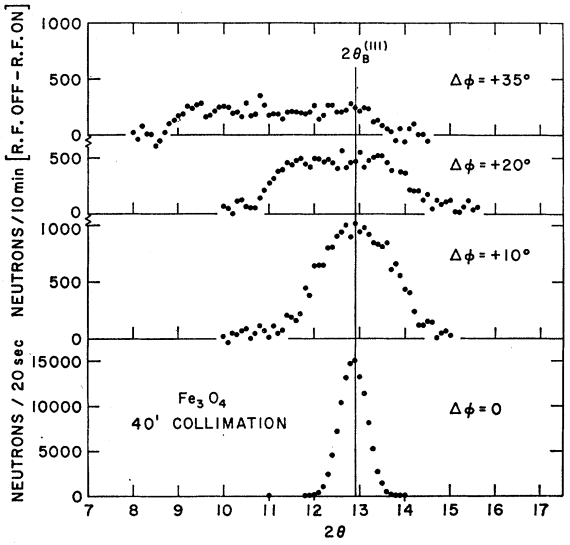

FIG. 3. The difference in intensities for the two states of neutron polarization for several angles of misset of the crystal from the Bragg position. The shift of the center of the profile from the Bragg position ($2\theta_B$) is a known function of the misset angle $\Delta\varphi$ and is denoted in Fig. 1 by the angle δ.

in a cryostat. The absolute value of the magnon scattering is much reduced because of the lower temperature. In addition there seems to be some elastic contamination due to the orthorhombic distortion. Nevertheless the difference plot of the data (Fig. 4) shows the characteristic magnon profile, although with much poorer statistics than the room-temperature measurements.

IV. DATA ANALYSIS

A. Resolution Correction

The ideal rectangular profile (angular width Γ) is convoluted with the resolution function (measured by fixing the crystal at the Bragg position and scanning the counter across the Bragg peak) to obtain a profile which can be compared with the observed difference counting rate (OFF-ON). The value of Γ was determined by varying this parameter until the best least squares fit was obtained between the calculated and observed profiles.[32] Figure 5 shows a typical result of fitting of the observed data. The points at the shoulders have greater weight than the other points in determining Γ. This fact is taken into account in ascribing an error to Γ. The average error on Γ for all measurements is approximately 1.5%.

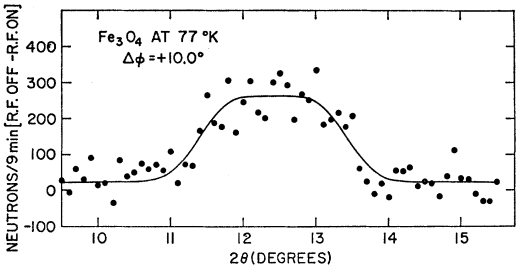

FIG. 4. One of the low-temperature profiles of the magnon scattering surface taken at a misset angle of 10.0°. The smooth curve is the best least-squares fit of the convolution of the resolution function with an ideal rectangular profile as explained in the text.

B. The Dispersion Curve

Since the experiment is performed by measuring Γ values as a function of the misset angle $\Delta\varphi$, the second task of the data analysis is to transform these results into an actual dispersion curve; i.e., to go from experimental space to energy–wave-vector ($\hbar\omega$,q) space.

Let us write the general dispersion law as

$$k_f^2 - k_i^2 = \epsilon f(q^2), \tag{12}$$

where we anticipate the function $f(q^2)$ to be a power series in q^2,

$$f(q^2) = \alpha q^2 + \beta q^4 + \gamma q^6 + \cdots \tag{13}$$

and $\epsilon = +1$ for magnon annihilation, $\epsilon = -1$ for creation.

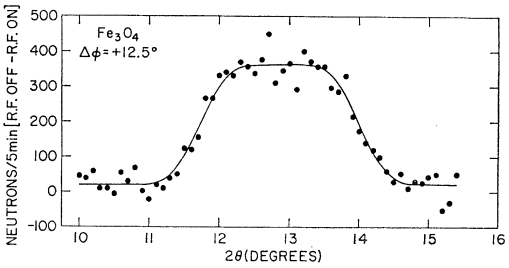

FIG. 5. A typical scan of the magnon scattering surface. The points are the difference in intensities for the two states of neutron polarization. The smooth curve shows the result of correcting for resolution effects as explained in the text. The angular width Γ of the ideal rectangular profile was determined in this case to be 2.29±0.05°.

As the neutron detector is scanned across the scattering surface (Fig. 1) with the crystal fixed at some misset angle $\Delta\varphi$, the angle Ψ that it makes with the vector $\mathbf{k}_1$ (fixed if $\Delta\varphi$ is fixed) changes. In so doing, the momenta of the neutrons scattered into the detector ($\mathbf{k}_f$) also changes in a way determined by the shape of the scattering surface. Now the particular angle $\Psi = \Gamma/2$ which gives the angular location of the steep shoulders of the observed profile is characterized by Ψ attaining its maximum value, i.e.,

$$d\Psi/dk_f = 0 \quad \text{when} \quad \Psi = \Gamma/2. \tag{14}$$

[32] Actually, four parameters were varied: Γ, a multiplicative scale factor, an additive constant, and the angular location of the center of the profile. This latter factor is determined by the geometry of the experiment (Ref. 27), so that it should be predictable. The average angular deviation of the observed center of the profile from the expected center was only 0.06 deg for the entire set of measurements.

From the scattering geometry (Fig. 1),

$$q^2=k_f^2+k_1^2-2k_1k_f\cos\Psi \qquad (15)$$

so that upon differentiating Eqs. (12) and (15) with respect to k_f and applying the condition (14) we obtain

$$k_f=-k_1(\cos\tfrac{1}{2}\Gamma)\epsilon g(q^2)/[1-\epsilon g(q^2)], \qquad (16)$$

where

$$g(q^2)\equiv(1/2q)[df(q^2)/dq].$$

The exact equations (12), (15), and (16) would enable one to solve for $(k_i/k_1)^2$ and $\sin^2(\Gamma/2)$ given a point $[f(q^2),q]$ on a known dispersion curve. Conversely, the equations show that if one wishes to transform from the $\sin^2\Gamma/2$ versus $(k_i/k_1)^2$ curve to the dispersion curve it is necessary to know the slope of the dispersion curve. Thus suggests an iterative procedure as follows: A good first approximation to the dispersion curve may be obtained by least-squares fitting a smooth curve through the experimental points which have been projected onto $(\hbar\omega,q)$ space by using Eq. (7). When the derivatives of the dispersion curve at these points are found, Eqs. (12), (15), and (16) then yield a corrected set of values for the experimental points in $(\hbar\omega,q)$ space. This process is repeated to convergence. It is convenient to take a power series in q^2 [Eq. (13)] for the fitting procedure. In this way starting with the quadratic term one may investigate whether the fit is improved by including higher powers of q^2. The approach used here was to terminate the procedure when the inclusion of higher powers of q^2 did not improve the fit.

TABLE I. Experimental results on the angular width Γ of the scattering surface.

Misset angle $\Delta\phi$ (deg)	$(k_i/k_1)^2$	Γ (deg)	$10^4\sin^2(\Gamma/2)$
	Room temperature		
0.5	1.004	0.65±0.02	0.32±0.02
5.0	1.040	1.42±0.02	1.53±0.04
7.5	1.061	1.84±0.03	2.57±0.07
10.0	1.083	2.01±0.04	3.08±0.09
10.0	1.083	1.98±0.04	3.00±0.09
12.5	1.105	2.29±0.05	4.0±0.1
−15.0	0.895	2.39±0.05	4.4 ±0.1
15.0	1.129	2.50±0.05	4.7 ±0.1
−20.0	0.865	2.66±0.08	5.4 ±0.2
17.5	1.151	2.72±0.04	5.6 ±0.1
−25.0	0.837	2.88±0.08	6.3 ±0.2
20.0	1.176	3.06±0.10	7.1 ±0.2
20.0	1.177	3.10±0.06	7.3 ±0.2
22.5	1.200	3.35±0.10	8.5 ±0.4
23.3	1.208	3.49±0.09	9.3 ±0.3
25.0	1.226	3.62±0.06	10.0 ±0.2
25.85	1.233	3.58±0.07	9.8 ±0.2
28.3	1.258	4.01±0.09	12.2 ±0.3
30.0	1.278	3.97±0.09	12.0 ±0.3
30.0	1.276	4.20±0.08	13.4 ±0.4
31.8	1.293	4.15±0.09	13.1 ±0.4
35.0	1.328	4.56±0.10	15.9 ±0.5
35.0	1.330	4.6 ±0.1	16.1 ±0.6
40.0	1.378	5.0 ±0.1	19.3 ±0.8
		77°K	
10.0	1.081	2.1 ±0.1	3.2 ±0.2
20.0	1.171	2.9 ±0.1	6.5 ±0.5

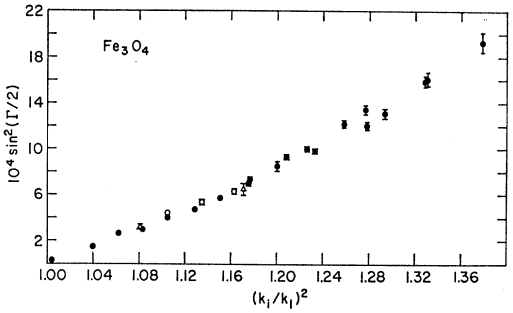

FIG. 6. The experimental data for the half angular width of the intensity profile (Γ/2) as a function of $\Delta\varphi$, the angle of misset of the crystal from the Bragg position. Instead of $\Delta\varphi$ directly, Γ/2 is plotted versus the quantity $(k_i/k_1)^2$ which is completely determined from a knowledge of k_i, the scattering geometry, and $\Delta\varphi$. The filled-in circles denote data taken at room temperature for $\Delta\varphi>0$ corresponding to magnon creation, and the open circles are for $\Delta\varphi<0$ (magnon annihilation). The triangles are data taken at 77°K.

V. RESULTS

Table I gives the results of the measurements of Γ, the angular width of the scattering surface (corrected for the effects of the resolution of the system as described above) for misset angles up to 40°, which was the practical limit that could be achieved with adequate counting statistics. The errors are taken from the resolution correction procedure. Figure 6 shows the data plotted in the form that would yield a straight line if the dispersion law were a quadratic function of q. This is evidently not the case. Figure 7 shows the dispersion curve obtained from the experimental results by the procedure just described. As expected, a decided improvement in the fit to the experimental points was obtained by including a q^4 term in the expansion of the energy, but because of the scatter in the data, no further improvement was obtained by including a q^6 term. The best smoothed dispersion curve can be expressed as:

$$\hbar\omega=(\hbar^2/2m)(\alpha q^2+\beta q^4) \qquad (17)$$

with $\alpha=297\pm15$ and $\beta=(-2.2\pm0.4)\times10^3$ Å^{-4} and is drawn as the dashed curve in Fig. 7.

The errors on α and β are estimated from the procedure used to arrive at the dispersion curve, taking into account the uncertainties in the experimental data, the effect of including a q^6 term, the scatter in the experimental points about the smooth curve, etc.

The agreement with the Ferguson *et al.*[24] measurements ($\alpha=234$) is excellent since we obtain a value of $\alpha=233$ if we should attempt to fit our results with a q^2 term only. However, this value is rather meaningless, since the dispersion law is in fact not quadratic in in this region.

For magnetite, the expression of the dispersion curve as a power series in q^2 over the limited range of q

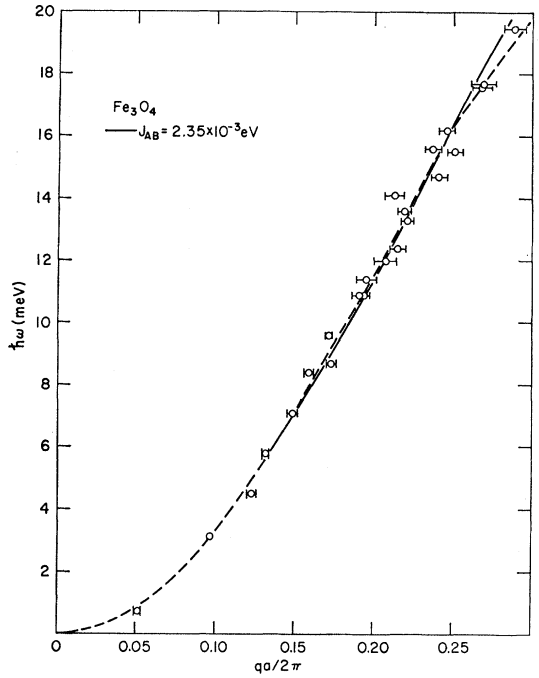

FIG. 7. The dispersion curve for Fe_3O_4 at room temperature. The experimental points shown have not been measured directly but are deduced from the data of Fig. 6 by the method explained in the text. The dashed curve is the best least-squares fit to the points taking an even power expansion in q up to power q^4. The solid curve gives the result of the Heisenberg theory (Ref. 17). It coincides with the dashed curve for the lower q values.

measured here is really of no interest since it can be compared directly with the prediction of the Heisenberg theory. From the work of Glasser and Milford[17] we have derived Eq. (3). The best fit to our results is given by taking $J_{AB}=2.35\times10^{-3}$ eV. and this is plotted in Fig. 7 as the full curve. It is evident that the agreement with theory is very good. The agreement with Brockhouse and Watanabe's measurements[4] by direct energy analysis is also good, and in fact within the range of q values measured here the errors of the diffraction method are less than those obtained from energy analysis.

The two measurements made at 77°K are shown on Fig. 6 where it is seen that there is no detectable departure of these measurements from those made at room temperature.

VI. CONCLUSIONS

The magnon scattering of polarized neutrons from magnetite has been measured for the acoustic branch for q vectors up to approximately one-third the zone boundary utilizing the diffraction method. Corrections were made for resolution and the results were transformed into a dispersion curve. The satisfactory agreement between these measurements and those of Brockhouse and Watanabe, as well as the good agreement with theory, leads to confidence in the diffraction method and the procedures used to reduce the data and express it as a dispersion curve. The greater accuracy of this method in the region of moderately small q vectors when compared to direct energy analysis leads one to conclude that in many cases this method will complement direct energy analysis in future investigations. This range of moderate q values is an interesting one. It is here where one may expect to find the effects of Kohn anomalies and phonon-magnon interactions, for example. The use of polarized neutrons for investigating these phenomena is especially appropriate.

The implications of the results of the measurements performed below the 119°K transition would seem to require that the cause of the discrepancy between the value of the exchange interaction deduced from the low-temperature specific-heat measurements[18] ($J_{AB}=0.44\times10^{-3}$ eV) and the room-temperature spin-wave measurements cannot be ascribed to some large change in the exchange interaction caused by the crystallographic distortion below this temperature. Rather, it would appear that the cause of the discrepancy must be sought in the calculations whereby one relates the specific heat to the dispersion curve.

Finally, it is well to reemphasize the fact that the insulating ionic ferromagnet Fe_3O_4 does indeed obey the Heisenberg theory. Recent measurements[12–14] on the metals Fe, fcc Co and hexagonal Co show decided departures from Heisenberg behavior.

Note added in proof. Heat-capacity measurements by M. Dixon, F. E. Hoare, and T. M. Holden [Phys. Rev. Letters **14**, 184 (1965)] yield a value for J_{AB} of $1.1\pm0.1\times10^{-3}$ eV, which is considerably higher than the Kouvel measurements cited in the text but still not high enough to agree with the neutron inelastic-scattering measurements. Inclusion of terms higher than q^2 in the heat-capacity calculation [R. P. Kenan, M. L. Glasser, and F. J. Milford, Phys. Rev. **132**, 47 (1963)] fail to alter the value of J_{AB} deduced therefrom. Furthermore, the recent renormalized magnon-spectra calculations of R. E. Mills, R. P. Kenan, and F. J. Milford [Phys. Rev. **145**, 704 (1966)] also yield results very close to the earlier linear-spin-wave theories,[16,17] so that the conclusions presented here are unchanged.